Journal of Engineering and Technological Advances (JETA)
https://jeta.segi.edu.my/index.php/segi
2025 Vol. 10 No. 1

DEVISING AN EFFECTIVE SILVER ION-CAPTURING SCAFFOLD WITH A CBD-SA LINKER-ENHANCED APTAMER: A SYNTHETIC BIOLOGY APPROACH

[1]Zhou, H., [2]Che, H., [3]Yao, G., [4]Fan, J., [5]Xu, Z., [5]Fan, H.S.*

[1] University of California, CA 95616, USA.

[2] Washington University in St. Louis, St. Louis, MO 63130, USA

[3] University of California San Diego, CA 92093-0021, USA

[4] Carnegie Vanguard High School, Houston, Texas, 77019, USA

[5] College of Chemical Engineering, Sichuan University of Science and Engineering, Zigong City, Sichuan Province, 643000, PR China

* Corresponding Author: fan27713@yahoo.com TEL: (86)-13755133052

Received: 29 April 2025; Accepted: 16 June 2025; Published: 30 June 2025

doi:10.35934/segi.v10i1.126

Highlights:

- Recycles silver ions from wastewater using a bioengineered protein system.
- Built with cellulose fibers, fusion proteins, and aptamers for capture.
- Maintains over 99% efficiency after 4 reuse cycles.

Abstract: Recycling is an important approach to preserving the world's valuable resources for the good and longevity of the planet, as well as to continue to live the way that humans are accustomed to. In this study, a silver ion capture and reusable platform was successfully assembled via a synthetic biology method to recycle metal ions in wastewater. Three modules exist in this platform: (1) a bacterial cellulose nanofiber block (BCNF), which is a structural module; (2) a fusion protein cellulose-binding domain (CBD) and streptavidin (SA)-based linker (CBD-SA-CBD); and (3) a biotin aptamer for metal ion capture blocks. The cellulose BCNF block showed the optimal glucose concentrations for cultivating the bacterial cellulose block. The optimal conditions were identified to induce proteins for the construction of the CBD-SA-CBD linker block. In general, the linker block binds effectively to the metal ion-capturing aptamer, and Aptamers 3 and 4 bind most effectively with silver ions. The reusability of this metal ion-catching aptamer maintained 99.16 to 99.56% binding affinity after four

repeated tests. The calculated silver binding efficiency (BE) of the complete assembly remained as high as 99.95%. This consistent binding affinity is a valuable asset in environmental applications. Owing to the diversity of aptamers and versatility of fusion proteins, this genetic engineering design has great potential for diverse future applications, such as heavy metals, antibiotics, pheromones, and even nuclear waste treatment and removal.

Keywords: Metal Ion Recycling; Bacterial Cellulose Nanofiber; Biotin-based Aptamer; Cellulose Binding Domain; Streptavidin

1. Introduction

Industrial and chemical contamination are a major problem under the industrialized society. The toxic heavy metals polluted the water system and the landscape through bioaccumulation and biomagnification processes (Blaha et al., 2011). Several countries encourage the reduction, reuse, and recycling (R^3) of metal waste (Hileman, 1999). Japan's e-waste initiative during the Tokyo Olympics was a typical example of R^3 efforts, where the medals were made by the e-waste program. Which leads to the consequences of not only saving more than $800,000 but also preventing metals from being released into the environment.

Several treatments involving metal ions in the environment have been developed. First, using an ion exchange resin is a low-cost, inexpensive, and efficient approach for water treatment. However, resin can only perform in harsh pH environments, which have to reprocess to adjust the pH (Cantwell et al., 1982). Second, precipitation is another chemical separation technique used to eliminate and collect specific pollutant ions from the effluent. Chemical precipitation of ions will form, which lead to drawbacks of expensive, non-reusable, and need further treatment to recover the precipitate in the compound or complex state to pure precious metals (Matlock et al., 2002). Third, ion-specific protein extraction is an biological treating technique, which proteins have been identified or modified to specifically bind to certain ions in water. However, it’s expensive and time-consuming to denature the protein after bound to the ion to reuse (Jung et al., 2020). A recent study by Jung et al. investigated an aptamer that could detect different metal ions in water. The Aptamer is an RNA sequence that can specifically bind to target molecule with positive charge by the electrostatic force with the negatively charged

phosphate backbone of the aptamer (Zhang et al., 2023). After detecting and binding to the target molecule, the single-stranded RNA folds into a vast set of tertiary structures, which can function like a clamp (Ng et al., 2006). Back to the research, aptamers can be used to bind various metal ions by slightly adjusting the sequences, which resulted in different structures and the ability to capture different metal ions. The research illustrates the potential of aptamer usage, which could not only identify different types of metal ions in water but also bind to and extract specific metal ions from water.

In this study, a synthetic biology approach was adopted to construct a reusable metal ion capture platform. There are three modules of this platform: 1) a bacterial cellulose nanofiber block (BCNF), 2) a cellulose-binding domain and streptavidin fusion protein (CBD-SA-CBD), and 3) a biotin aptamer. To decrease the contamination of the product, we choose cellulose, the environmentally friendly materials, as a baseline of our system, which is biocompatible, biodegradable and widely sourced biomass material. The cellulose-binding domain (CBD) can interact with cellulose through non-covalent bonds and bring linked catalytic protein domain(s) to the surface of the substrate to enhance enzyme activity. The CBD has the characteristic of high specificity, highly efficient and low-cost (Liu et al., 2021). Between biotin and streptavidin fusion protein (SA), the strong non-covalent bond, hydrogen bond and Van der Waals contacts stabilized the connection of the two molecules (Ayan et al., 2022). Our system chose to target the Ag+ ion because recycled silver ions can be used for many purposes, especially in medicine (Zhang et al., 2020; Zhang & Wang, 2018). We also used silver ions to test the efficiency of the aforementioned ion capture–recycle platform. The ion capture platform with captured silver is heated to release the metal ions. The reusability of the platform was tested for its binding ability after multiple heating cycles. The specificity and binding efficiency of metal ions will be characterized by ICP–MS, an analytical environmental testing technique. The reusability and selectivity of such an aptamer-based platform will provide a unique synthesis route to prepare an effective metal ion R3 candidate. By using only biology-derived components, this ion capture-recycling device will have no significant impact on the environment, nor will it need costly or complicated posttreatment. Owing to the diversity and versatility of the aptamers

and fusion proteins, this genetic engineering design could be applied to many other areas in the future, including heavy metals, antibiotics, pheromones, and even nuclear waste treatments.

2. Materials and Methods

2.1. Bacterial Strains and Culture Conditions

All strains of bacteria used in the study are listed in **Table 1**.

Table 1. Strains, plasmids, and aptamers used in the study

Strain, Plasmid, and Aptamers		Description	Source
Strains	***E.coli* DH5$^{\alpha}$**	For plasmid storage	Lab Stock
	***E.coli* BL21**	Protein Production	Lab Stock
	***A.xylinum* ATCC23767**	For cellulose production	Bought from Huzbio
Plasmids	**pET28b**	PTac, rop, KanR, f1 ori, T7, MCS	Lab Stock
	SHS1	pET28b derivative, Fus-CEC	This Study
	SHS2	pET28b derivative, Fus-CSC	This Study
Aptamers	**A1**	Ag^{+} Aptamer, Vb7	Zhou et al. (2020)
	A2	Ag^{+} Aptamer, Vb7	Shen et al. (2020)
	A3	Ag^{+} Aptamer, Vb7	Shen et al. (2020)
	A4	Ag^{+} Aptamer, Vb7	Shen et al. (2020)
	A5	Ag^{+} Aptamer, Vb7	Lin et al. (2011)
	A6	Ag^{+} Aptamer, Vb7	Lin et al. (2011)
	A7	Ag^{+} Aptamer, Vb7	He et al. (2012)
	A8	Ag^{+} Aptamer, Vb7	Cai et al. (2018)
	A9	Ag^{+} Aptamer, Vb7	Saran et al. (2018)
	A10	Ag^{+} Aptamer, Vb7	Saran et al. (2018)
	C1	Control Aptamer, Vb7	Saran et al. (2018)
	AF	FITC, poly A, Vb7	Saran et al. (2018)

2.2. Plasmid Construction

The plasmids used in the study are listed in **Table 1**. The fusion genes (Fus-CEC and Fus-CSC) were purchased from Hitrobio. The promoters and terminators used in the study were provided in the pET28b plasmid, which was stored in the laboratory.

The plasmids SHS1 and SHS2 were both created from the pET28b plasmid and were purchased from Hitrobio.

2.3. Aptamer Selection

Ten aptamers (**Table 1**) and the control aptamer were obtained from previous literature and were purchased with VitaminB7 (Vb7) at the 5' end from Hitrobio. Studies have shown that different aptamers have different binding abilities to silver ions (Golovlev et al., 2001; He et al., 2012; Jung et al., 2020; Lin et al., 2011; Saran et al., 2018; Shen et al., 2020; Zhou et al., 2020). This study selected ten different aptamers to investigate their binding efficiencies toward silver ions (shown in **Figure 6**). The detailed preparation and storage procedures of aptamers were based on previous literature (Lin et al., 2011).

2.4. Protein Expression and Purification

The expression and purification procedures for both Fus-CEC and Fus-CSC is given here (Bartels et al., 2018). We designed three trials of the experiment to find out the optimal kana solution concentration, temperature, and IPTG concentration.

2.5. Cellulose Production

The procedure of bacterial celluose production using *A. xylinum* was based on previous article (Li et al., 2020). After production, the cellulose was removed, weighed, and air dried for 2 hours. The dried cellulose was then weighed again.

2.6. SA-aptamer Interaction Test

Different volumes of the SA and MOPS solutions (**Table 2**) were transferred into 10 µl of AF aptamer at 100 µM. The systems were then set aside for half an hour and shaken every five minutes. The systems were subsequently centrifuged at 12,000 rpm for 5 minutes before 70 µl of the supernatant from each mixture was added to 80 µl of 50 mM MOPS at pH 7.2. The

resulting solutions were then tested for fluorescence with excitation at 495 nm and emission at 519 nm. For each volume for the SA and MOPS solutions, 5 repeats had been tested. The binding efficiency (BE) of each system was subsequently calculated via equation 1.

$$BE = \frac{Control\ florescence - Tested\ florescence}{Control\ florescence - Background\ florescence} \quad (1)$$

Table 2. Streptavidin-biotin interaction test

Aptamer/ul	10	10	10	10	10	0
50mM 7.2 MOPS/ul	100	99	95	80	0	10
SA beads/ul	0	1	5	20	100	100

2.7. CBD Domain–Cellulose Interaction Test

Four 2 ml solutions of 0.5% cellulose powder were taken and centrifuged at 12,000 rpm for 10 minutes, the supernatant was discarded, and the mixture was resuspended in 2 ml of 50 mM MOPS pH 7.2 solution. The solutions were subsequently divided into one control group and three experimental groups (**Table 3**). Within each group, there was one positive tube with the cellulose suspension and one without it; 10 µl of the Fus-CFC protein was added to each tube before being placed in a 4°C freezer for one hour, and the tubes were shaken every five minutes. After an hour, the tubes were centrifuged at 12,000 rpm for 10 minutes, and the samples were tested for the fluorescence of the supernatants and calculated for the BE.

Table 3. CBD domain-cellulose test

	Control		**G1**		**G2**		**G3**		**G4**	
	+	-	+	-	+	-	+	-	+	-
CFC/µl	0	0	10	10	5	5	2	2	1	1
Suspension/ml	2	0	2	0	2	0	2	0	2	0
MOPS/ml	0	2	0	2	0	2	0	2	0	2

2.8. System Test

Prepared 5 tubes, each tube with 5 µl of Fus-CSC protein, 20 µl of aptamer 4, 50 µl of 100 µM Ag^{+} solution, and 925 µl of MOPS buffer were added to one EP tube, with another system

created in another tube using a control aptamer instead. The systems then went through the aptamer selection procedure, and the ion concentration was tested with ICP–MS again.

2.9. Reusability Test

The chosen aptamer (A4)-prepared 100 μl solution was subjected to the aptamer selection procedure again. However, at the end of the procedure, the sediment was not discarded but was heated to 80°C for 30 minutes before being centrifuged again at 12,000 rpm for 5 minutes, after which the sediment was preserved. The above procedure is subsequently repeated two times for the sediment. Each time, the silver ion concentration of the supernatant was tested via ICP–MS.

3. Results and Discussion

To collect and recycle silver ions in industrial wastewater, a metal ion capture-recycling platform was designed on the basis of the synthetic biology concept. **Figure 1** shows the mechanism of three components in our silver ion extraction system.

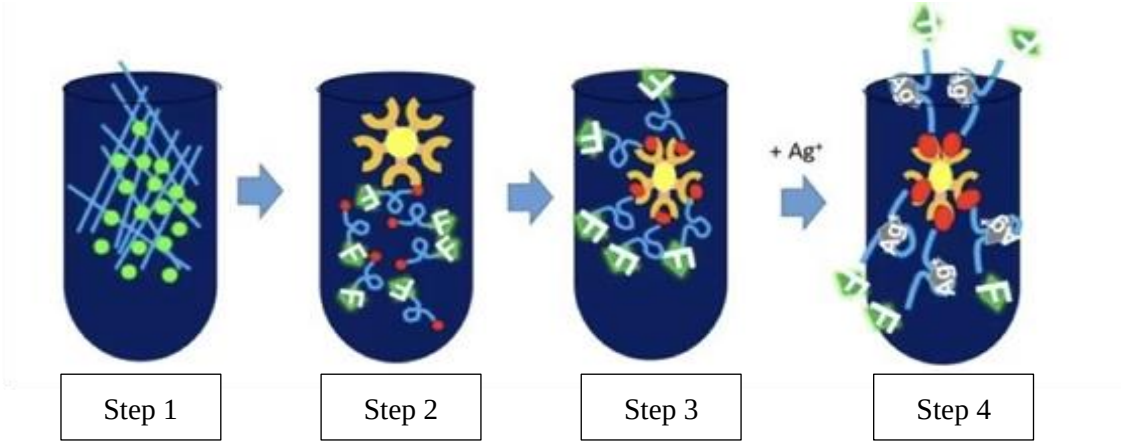

Figure 1. Overview of the metal ion capture-recycling platform including the three components: BCNF, CBD-SA-CBD and biotin aptamer. Step 1: Binding between Cellulose and CBD-SA. Step 2: Construction of CBD_SA_CBD block and biotin-aptamer. Step 3: Connecting CBD-SA-CBD block and aptamer. Step 4: Binding between biotin-aptamer and silver ions

We assembled the three-block platform and tested the binding efficiency of silver ions in the industry effluents. The following section details the construction and characterization of each block.

3.1. Construction of the BCNF Block

The key ingredient of BCNF is *Acetobacter xylinum* (Hamad et al., 2023). The BCNF block stands as a structural module in the platform due to the structural support of the platform when connecting to the other two blocks. Assuring the quality and yield of the bacterial cellulose is important (Li et al., 2020). To investigate the quality and yield of cellulose, we tested four different culture media to determine the optimal conditions for bacteria to produce cellulose.

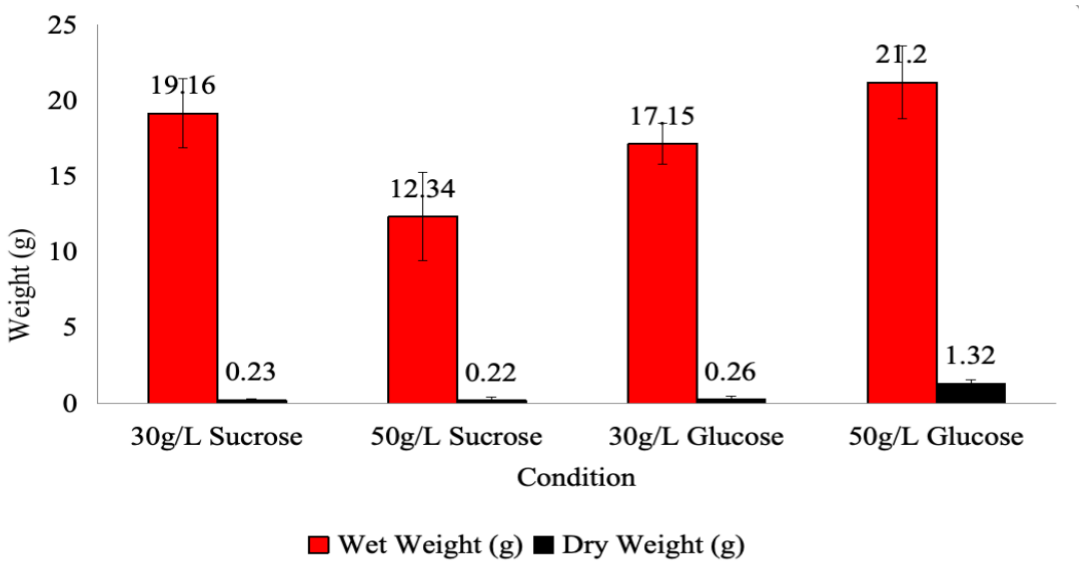

Figure 2. Wet weight and dry weight of bacterial cellulose yield from four different culture media

Figure 2 shows the wet and dry weights of the bacterial cellulose yields from the four different culture medias. The specific pattern of different concentrations and types of sugar to yield for a higher weight of cellulose are not shown by **Figure 2**. However, group 4(50 g/L glucose) in **Figure 2** shows the heaviest wet weight and dry weight, and the smallest weight difference between the wet and dry weights. This small weight difference suggests that a carbon source from 50 g/L glucose is the optimal condition for cultivating bacterial cellulose.

3.2. Construction and Characterization of the CBD-SA Block

A linker module, CBD-SA-CBD, connects the bacterial cellulose BCNF block and the ion-capturing biotin-aptamer block. The connection is based on a fusion protein that contains two

cellulose-binding domains and one streptavidin domain, which is produced by genetically engineered *B. subtilis* (Bartels et al., 2018; Janc et al., 2021).

To find the best protein-inducing conditions to construct the fusion protein block, we designed three trials of experiment to find out the optimal kana solution concentration, temperature, and IPTG concentration. The fluorescence readings of all the samples used to measure optical density were collected and compared. The results revealed that samples without kana, under incubated temperature 24°C and IPTG concentration 0.05 mM presented brighter fluorescence than samples with kana, under incubated temperature 16°C and IPTG concentration other than 0.05 mM. This result suggested that more proteins were synthesized in samples with kana, at incubated temperature 24°C, and, interestingly, the 0.05 mM concentration of IPTG but not higher concentration, because the cellulose becomes sticky when the concentration is too high, making the induced protein less effective. Therefore, the optimal conditions of 0.05 mM IPTG, 24°C, and no kana addition are needed to induce the most protein for the construction of the CBD-SA-CBD block.

3.3. The BCNF and Linker Blocks are Connected

To find out the optimal conditions to connect the cellulose BCNF block and the linker CBD-SA-CBD block, we altered the cellulose concentration and eGFP concentration. Six groups of different cellulose concentrations were used (as shown in **Table 4**). Then, the resulting fluorescence value of each group was collected to calculate the binding efficiency between these two blocks. The control group (group #6) contained 0% cellulose. As shown in **Table 4**, the eGFP group was used in place of SA in the CBD-SA-CBD block because eGFP has properties similar to those of SA and is a visible fluorescent marker (Barnard & Timson, 2010).

The precipitate will form if cellulose binds with the CBD-eGFP-CBD block, so we can examine the concentration of protein and calculate the binding efficiency by detecting the change in fluorescence upon binding. **Figure 3** shows the binding efficiency between the cellulose and linker blocks at various cellulose concentrations, and the vertical lines on the graph indicate the margin of error. The binding efficiency increases when the cellulose concentration is between 0% and 0.5%, indicating that the cellulose block can bind effectively with the linker block. The

BE is relatively high when the concentration of cellulose is 0.2% or 0.5%. Because the cellulose becomes sticky when the concentration gets higher, it will interfere with the interaction between cellulose and linker block, so the binding efficiency decreases when the cellulose concentration is greater than 0.5% (Barbosa et al., 2021). Thus, a 0.2% cellulose concentration was selected for the subsequent investigation.

Table 4. Samples with different concentrations of cellulose

Samples	**1**	**2**	**3**	**4**	**5**	**6**
Cellulose Concentration	2%	1%	0.5%	0.2%	0.1%	control
Cellulose Volume (mL)	2	2	2	2	2	2
CBD-eGFP-CBD (μg)	2	2	2	2	2	0

In **Figure 3**, by ANOVA test, the F statistic is 17.684 and the p-value is 1.508*10-5, which is smaller than alpha=0.50. We reject the null hypothesis that there is no difference within different concentrations and can conclude that concentration affects the binding efficiency. As the substituent for the SA moiety, the optimal eGFP concentration for the binding efficiency between cellulose and CBD-SA-CBD blocks was also tested using similar procedures. **Figure 4** shows that the binding efficiency of eGFP increased when the amount of eGFP was increased from 0 to 5 μg. The binding efficiency then plateaued and increased slightly from 69.93% at 5 μg to 71.98% at 10 μg. Therefore, a concentration of 10 μg of eGFP was used in subsequent investigations.

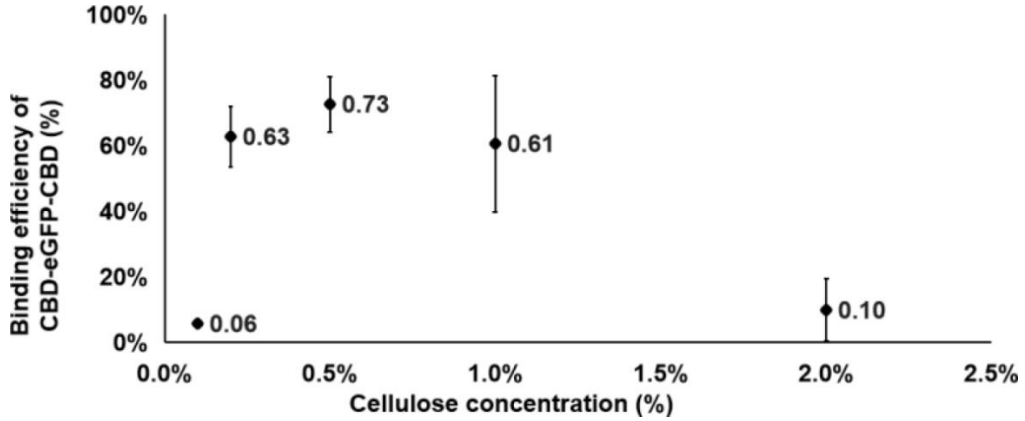

Figure 3. Binding efficiency of CBD-SA to cellulose at different cellulose concentrations

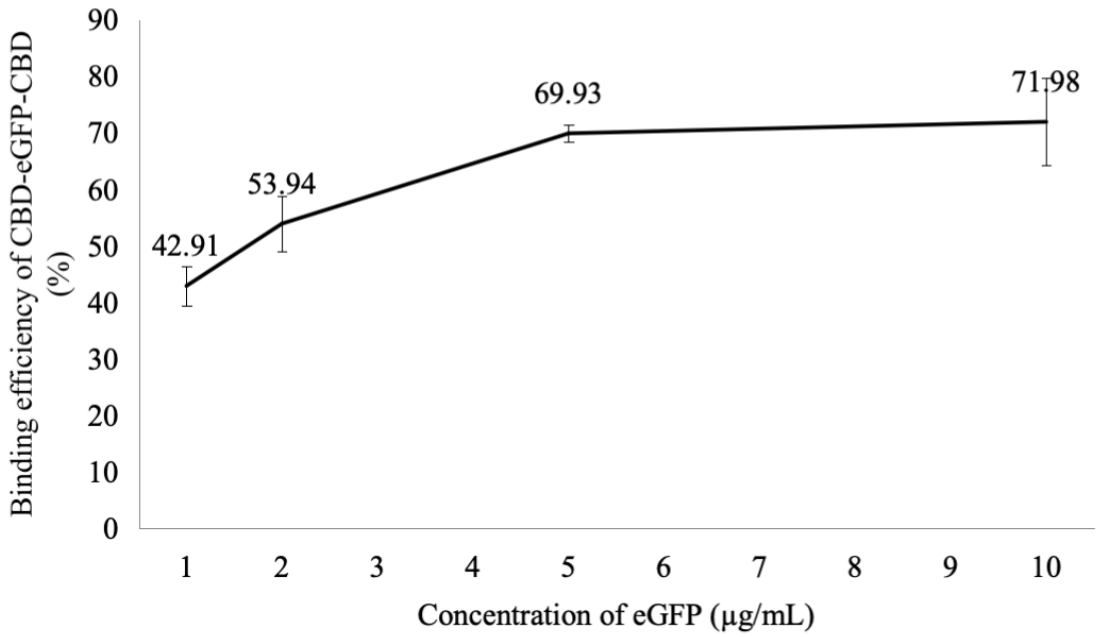

Figure 4. Relationship between the concentration of eGFP and the binding efficiency

3.4. Construction of a Metal Ion Binding Block

An aptamer-based ion binding block is the third component and the key structure of the ion capture–recycle platform. It is the biotin-modified DNA sequence which is capable of binding to metal ions (Shen et al., 2020; Xie et al., 2023). Two factors that might affect aptamer's effectiveness were considered: the concentration of the linker block and the incubated temperature of aptamer (Lin et al., 2016; Yan et al., 2019). The temperature is an important factor because if the temperature is too high, the protein can denature; in contrast, if the temperature is too low, the metal ions cannot be released (Bhargava et al., 2018).

We first attached a luminescent substance called FAM to the aptamer, which enables the detection of the ion-catching block upon its connection to the fusion protein linker block and calculation of the amount of aptamer that was successfully connected to the linker block (Yan et al., 2020; Zhang et al., 2020). Second, to investigate the connection between the ion-catching block and the linker block, samples with different concentration of components were used (as shown in **Table 2**). The magnetic bead was used in place of the CBD-SA-CBD linker block to better separate the ion-capture block after binding the linker block. In addition to the different concentrations of beads, two different temperatures (4°C and room temperature) were used in the experiments. The results were shown in **Figure 5**. Because of the centrifugation, the

aggregates of the linker and ion-catching block should be removed, and the luminescent FAM moiety should be extracted from the solution with the beads. The lower fluorescence readings of a solution indicate a more efficient aptamer. In **Figure 5**, the binding efficiency between beads and aptamers is represented as the ratio of decrease in the fluorescence readings and the original fluorescence readings. In general, the binding efficiency of the ion-catching aptamer block continued to improve as the number of beads increased from 0 to 100 μL at both 4°C and room temperature. These results suggested that the fusion protein CBD-SA-CBD linker block effectively bound to the aptamer.

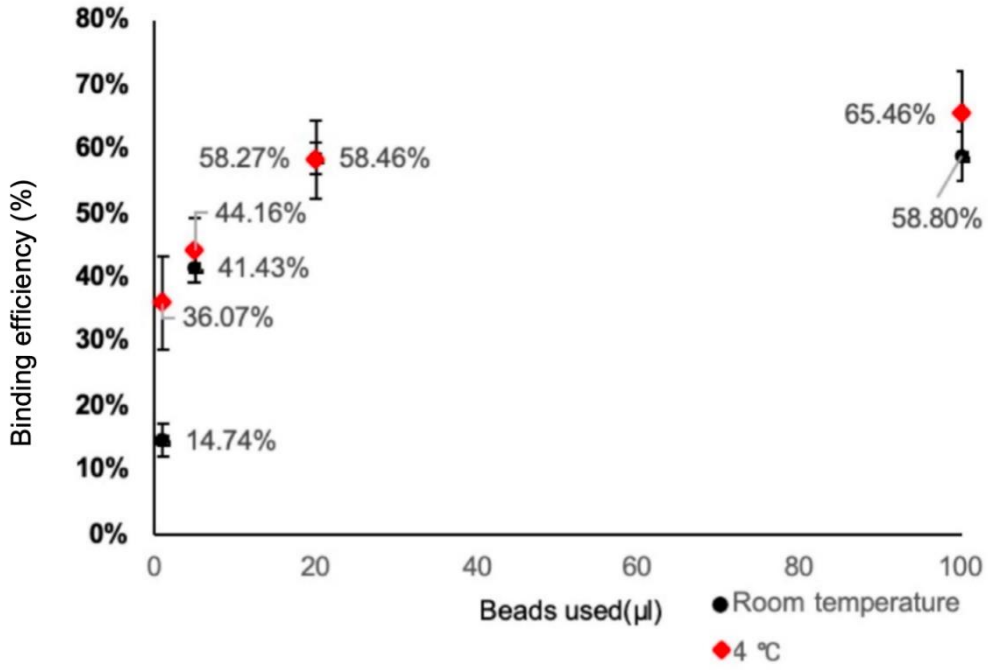

Figure 5. Binding efficiency between beads and aptamers at 4°C and room temperature

By performing a two-way ANOVA test for **Figure 5**, the F statistic is 8.1855, and the p-value is 0.0003482, which is smaller than alpha=0.50. We can conclude that there is a statistically significant interaction effect between beads' concentration and temperature change on the binding efficiency.

3.5. Binding the Silver Ion

In **Figure 6**, the ability of the ion-catching block to congregate silver ions in industrial effluents was investigated by detecting the free silver ions remained in the solution. For **Figure 6**, be performing single factor ANOVA test, the F statistic is 48.113 and the p-value is 2.2*10-16,

which is smaller than alpha=0.50. We reject the null hypothesis that there is no difference within different aptamer types and can conclude that the aptamer affects the concentration of silver ions.

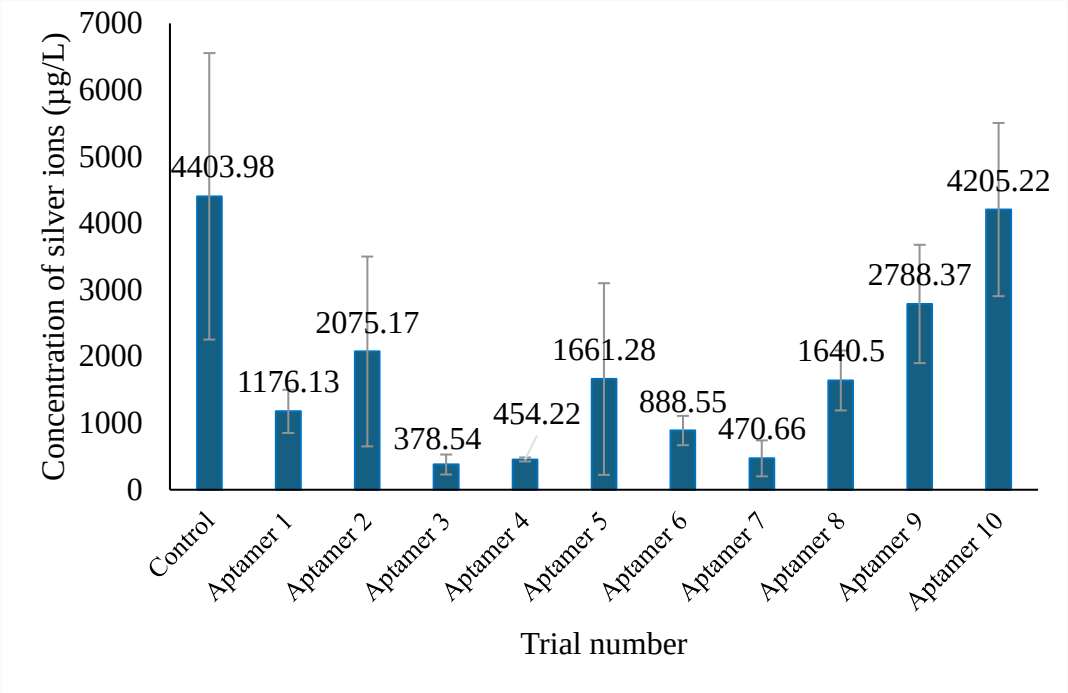

Figure 6. Concentration of the remaining Ag^{+} ions in the liquid supernatant (mean ± SE) after being captured by different aptamers. The dotted line indicates the initial Ag^{+} concentration before the aptamers were added

Compared with the control, the original Ag^{+} ion concentration, only a small decrease was detected in the aptamer 10 solution, which was the least effective at capturing Ag^{+} ions. On the other hand, aptamers 3 and 4 bound most effectively with silver ions, by showing more than 90% of the Ag^{+} ions being removed from the solution. According to the result shown in **Figure 6**, the order of the binding efficiency of the aptamers to Ag^{+} ions follows: aptamers 3 > 4 > 7 > 6 > 1 > 8 > 5 > 2 > 9 > 10. In addition, the CD spectrometer from Shen et al. The data shows that both the Cy3 emission(570nm) and Cy5 emission(660nm) are enhanced with the addition of Ag^{+}, which suggests that the aptamer interacts and aggregates with the Ag^{+}.

3.6. The Reusability of the System

The reusability of the ion-catching aptamer is another important indicator of successful metal ion capture and recycling (Christianson & Waters, 2021). To test reusability, the ion-catching

experiment described in the previous section was repeated four times. In **Figure 7**, the four repeat trials all showed 99.16% to 99.56% binding efficiency between aptamer and silver ions. We can conclude that the reusability of the Ag^{+} aptamer has consistency, and the binding efficiency toward silver ions remains remarkably high, even after being reused four times. The reusability of this ion capture–recycle platform and silver ion is attractive for future studies.

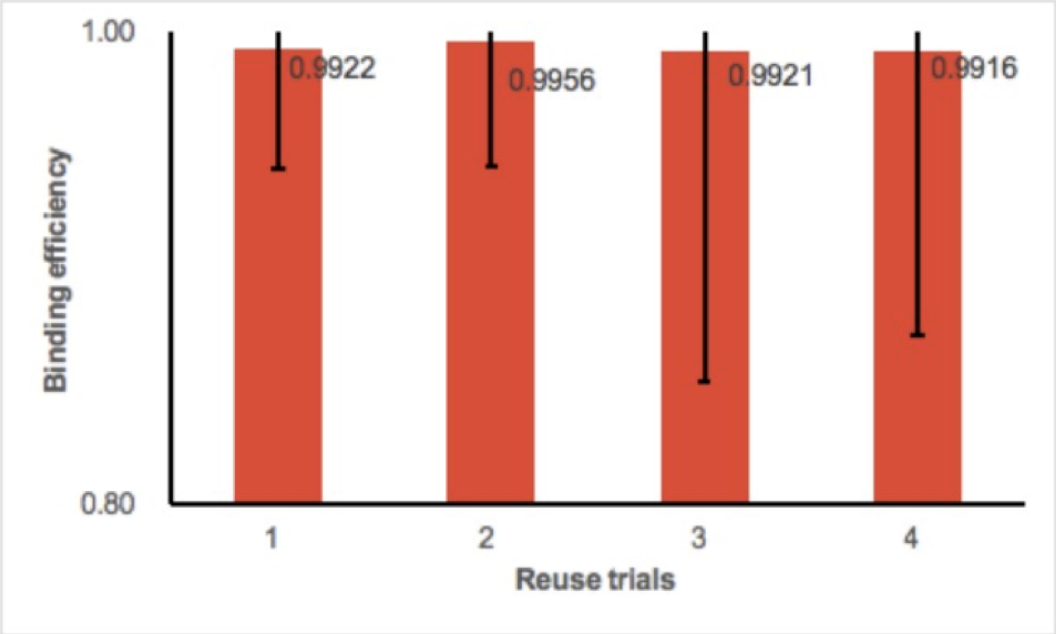

Figure 7. Binding efficiency of the aptamer to silver ions in four reuse trials

3.7. Testing of the Complete System

To test the efficiency of complete assembly for Ag^{+} binding and release/recycling, a concentration of initial silver ions of 428.16 μg/L was used in both the control and experimental groups. Result shows that only 0.2 μg/L of silver ions remained in solution after binding. The calculated silver binding efficiency of the complete assembly was 99.95%.

3.8. Comparing the Silver Ion Binding Efficiency between our System and Conventional Methods

Our system has an efficiency of 99.95%, which surpasses the three other conventional methods: the ion exchange resin(80-95%), chemical precipitation(30-70%) and ion-specific protein extraction(90-95%) (Fu & Wang, 2011). Thus, the percentage of selectivity for our system is the highest among all four silver ion extraction method.

4. Conclusion

In this study, a reusable silver ion capture platform was assembled to recycle metal ions from wastewater via a synthetic biology method. There are three modules in this assembly: a bacterial cellulose nanofiber block (BCNF), a cellulose binding domain and streptavidin fusion protein (CBD-SA-CBD), and a biotin aptamer. Each module was synthesized and tested for functionality before assembly. The optimal conditions of culturing and producing each module were found. The aptamer efficiency had been selected and concluded to use aptamer 3 and 4. The reusability of the silver ion capture system was high after 4 repeated trials. Owing to the high reusability, diversity and versatility of the aptamers and the fusion protein, this genetic engineering design has great potential for applications such as heavy metals, antibiotics, pheromones, and even nuclear waste treatment methods and removal.

Acknowledgement

We thank Chuan Ni and Cheng Li for their inspiration of the research topic and the experimental design. Also, we thank for the SHSBNU iGEM team for constructing the experiments together.

Credit Author Statement

Conceptualization, Z.H., C.H. and Y.G.; methodology, C.H.; validation, Z.H., C.H. and Y.G.; formal analysis, Y.G.; investigation, Y.G., C.H. and Z.H.; resources, Z.H.; data curation, Y.G.; writing—original draft preparation, Z.H., C.H. and Y.G.; writing—review and editing, Z.H., Y.G. and F.J.; visualization, Y.G., H.S. and X.Z.; supervision, H.S.; project administration, H.S.

Conflict of Interest

The authors declare no conflicts of interest.

References

Ayan, E., Yuksel, B., Destan, E., Ertem, F. B., Yildirim, G., Eren, M., Yefanov, O. M., Barty, A., Tolstikova, A., & Ketawala, G. K. (2022). Cooperative allostery and structural dynamics of streptavidin at cryogenic-and ambient-temperature. *Communications biology*, *5*(1), 73. https://doi.org/10.1038/s42003-021-02903-7

Barbosa, M., Simões, H., & Prazeres, D. M. F. (2021). Functionalization of cellulose-based hydrogels

with bi-functional fusion proteins containing carbohydrate-binding modules. *Materials*, *14*(12), 3175. https://doi.org/10.3390/ma14123175

Barnard, E., & Timson, D. J. (2010). Split-EGFP Screens for the Detection and Localisation of Protein–Protein Interactions in Living Yeast Cells. *Molecular and Cell Biology Methods for Fungi*, 303-317. https://doi.org/10.1007/978-1-60761-611-5_23

Bartels, J., López Castellanos, S. n., Radeck, J., & Mascher, T. (2018). Sporobeads: The utilization of the Bacillus subtilis endospore crust as a protein display platform. *ACS synthetic biology*, *7*(2), 452-461. https://doi.org/10.1021/acssynbio.7b00285

Bhargava, A., Pareek, V., Roy Choudhury, S., Panwar, J., & Karmakar, S. (2018). Superior bactericidal efficacy of fucose-functionalized silver nanoparticles against Pseudomonas aeruginosa PAO1 and prevention of its colonization on urinary catheters. *ACS applied materials & interfaces*, *10*(35), 29325-29337. https://doi.org/10.1021/acsami.8b09475

Blaha, U., Basavaiah, N., Deenadayalan, K., Borole, D., & Mohite, R. (2011). Onset of industrial pollution recorded in Mumbai mudflat sediments, using integrated magnetic, chemical, 210Pb dating, and microscopic methods. *Environmental science & technology*, *45*(2), 686-692. https://doi.org/10.1021/es1025905

Cai, S., Yan, J., Xiong, H., Liu, Y., Peng, D., & Liu, Z. (2018). Investigations on the interface of nucleic acid aptamers and binding targets. *Analyst*, *143*(22), 5317-5338. https://doi.org/10.1039/C8AN01467A

Cantwell, F. F., Nielsen, J. S., & Hrudey, S. E. (1982). Free nickel ion concentration in sewage by an ion exchange column-equilibration method. *Analytical Chemistry*, *54*(9), 1498-1503. https://doi.org/10.1021/ac00246a012

Christianson, A. M., & Waters, C. A. (2021). Silver chloride waste recycling as a guided-inquiry experiment for the instrumental analysis laboratory. *Journal of Chemical Education*, *99*(2), 1014-1020. https://doi.org/10.1021/acs.jchemed.1c00871

Fu, F., & Wang, Q. (2011). Removal of heavy metal ions from wastewaters: A review. *Journal of Environmental Management*, *92*(3), 407-418.

https://doi.org/https://doi.org/10.1016/j.jenvman.2010.11.011

Golovlev, V., Lee, S., Allman, S., Taranenko, N., Isola, N., & Chen, C. (2001). Nonresonant MALDI of oligonucleotides: Mechanism of ion desorption. *Analytical Chemistry*, *73*(4), 809-812. https://doi.org/10.1021/ac001006

Hamad, A., Giswantara, G., Pusapawiningtyas, E., Pamungkas, R. B., & Mulyadi, A. H. (2023). Optimization Of process parameters for microbial cellulose production from rice-washing wastewater (NATA-DE-LERI) By Acetobacter Xylinum. *Techno (Jurnal Fakultas Teknik, Universitas Muhammadiyah Purwokerto)*, *24*(1), 51-58. https://doi.org/10.30595/techno.v24i1.16988

He, X., Qing, Z., Wang, K., Zou, Z., Shi, H., & Huang, J. (2012). Engineering a unimolecular multifunctional DNA probe for analysis of Hg 2+ and Ag+. *Analytical Methods*, *4*(2), 345-347. https://doi.org/10.1039/C2AY05823E

Hileman, B. (1999). EU, US clash over environmental policies-Conflicts over climate change, biotech crops, and beef hormones are leading to difficult negotiations, trade wars. In (Vol. 77, pp. 21-26): AMER CHEMICAL SOC 1155 16TH ST, NW, WASHINGTON, DC 20036 USA.

Janc, T., Korb, J.-P., Luksic, M., Vlachy, V., Bryant, R. G., Mériguet, G., Malikova, N., & Rollet, A.-L. (2021). Multiscale water dynamics on protein surfaces: protein-specific response to surface ions. *The Journal of Physical Chemistry B*, *125*(31), 8673-8681. https://doi.org/10.1021/acs.jpcb.1c02513

Jung, J. K., Alam, K. K., Verosloff, M. S., Capdevila, D. A., Desmau, M., Clauer, P. R., Lee, J. W., Nguyen, P. Q., Pastén, P. A., & Matiasek, S. J. (2020). Cell-free biosensors for rapid detection of water contaminants. *Nature biotechnology*, *38*(12), 1451-1459. https://doi.org/10.1038/s41587-020-0571-7

Li, Q., Ma, Q., Wu, Y., Li, Y., Li, B., Luo, X., & Liu, S. (2020). Oleogel films through the Pickering effect of bacterial cellulose nanofibrils featuring interfacial network stabilization. *Journal of Agricultural and Food Chemistry*, *68*(34), 9150-9157. https://doi.org/10.1021/acs.jafc.0c03214

Lin, Y., Zhou, Q., Tang, D., Niessner, R., Yang, H., & Knopp, D. (2016). Silver nanolabels-assisted ion-

exchange reaction with CdTe quantum dots mediated exciton trapping for signal-on photoelectrochemical immunoassay of mycotoxins. *Analytical Chemistry*, *88*(15), 7858-7866. https://doi.org/10.1021/acs.analchem.6b02124

Lin, Z., Li, X., & Kraatz, H.-B. (2011). Impedimetric immobilized DNA-based sensor for simultaneous detection of Pb2+, Ag+, and Hg2+. *Analytical Chemistry*, *83*(17), 6896-6901. https://doi.org/10.1021/ac2014096

Liu, Z., Lin, D., Shen, R., & Yang, X. (2021). Bacterial cellulose nanofibers improved the emulsifying capacity of soy protein isolate as a stabilizer for pickering high internal-phase emulsions. *Food Hydrocolloids*, *112*, 106279. https://doi.org/10.1016/j.foodhyd.2020.106279

Matlock, M. M., Howerton, B. S., & Atwood, D. A. (2002). Chemical precipitation of lead from lead battery recycling plant wastewater. *Industrial & engineering chemistry research*, *41*(6), 1579-1582. https://doi.org/10.1021/ie010800y

Ng, E. W., Shima, D. T., Calias, P., Cunningham Jr, E. T., Guyer, D. R., & Adamis, A. P. (2006). Pegaptanib, a targeted anti-VEGF aptamer for ocular vascular disease. *Nature reviews drug discovery*, *5*(2), 123-132. https://doi.org/10.1038/nrd1955

Saran, R., Yao, L., Hoang, P., & Liu, J. (2018). Folding of the silver aptamer in a DNAzyme probed by 2-aminopurine fluorescence. *Biochimie*, *145*, 145-150. https://doi.org/10.1016/j.biochi.2017.07.001

Shen, F., Mao, S., Mathivanan, J., Wu, Y., Chandrasekaran, A. R., Liu, H., Gan, J., & Sheng, J. (2020). Short DNA oligonucleotide as a Ag+ binding detector. *ACS omega*, *5*(44), 28565-28570. https://doi.org/10.1021/acsomega.0c03372

Xie, Y., Yang, M., Zhu, L., Yue, X., Zhai, B., & Xu, W. (2023). Research progress of DNA aptamer-based silver ions detection. *Advanced Agrochem*, *2*(3), 231-235. https://doi.org/10.1016/j.aac.2023.06.006

Yan, N., He, X., Tang, B. Z., & Wang, W.-X. (2019). Differentiating silver nanoparticles and ions in medaka larvae by coupling two aggregation-induced emission fluorophores. *Environmental science & technology*, *53*(10), 5895-5905. https://doi.org/10.1021/acs.est.9b01156

Yan, N., Tsim, S. M. J., He, X., Tang, B. Z., & Wang, W.-X. (2020). Direct visualization and quantification of maternal transfer of silver nanoparticles in zooplankton. *Environmental science & technology*, *54*(17), 10763-10771. https://doi.org/10.1021/acs.est.0c03228

Zhang, H.-L., Lv, C., Li, Z.-H., Jiang, S., Cai, D., Liu, S.-S., Wang, T., & Zhang, K.-H. (2023). Analysis of aptamer-target binding and molecular mechanisms by thermofluorimetric analysis and molecular dynamics simulation. *Frontiers in Chemistry*, *11*, 1144347. https://doi.org/10.3389/fchem.2023.1144347

Zhang, L., Jiang, H., & Wang, W.-X. (2020). Subcellular imaging of localization and transformation of silver nanoparticles in the oyster larvae. *Environmental science & technology*, *54*(18), 11434-11442. https://doi.org/10.1021/acs.est.0c03342

Zhang, L., & Wang, W.-X. (2018). Dominant role of silver ions in silver nanoparticle toxicity to a unicellular alga: evidence from luminogen imaging. *Environmental science & technology*, *53*(1), 494-502. https://doi.org/10.1021/acs.est.8b04918

Zhen, H., Wu, X., Hu, J., Xiao, Y., Yang, M., Hirotsuji, J., Nishikawa, J.-i., Nakanishi, T., & Ike, M. (2009). Identification of retinoic acid receptor agonists in sewage treatment plants. *Environmental science & technology*, *43*(17), 6611-6616. https://doi.org/10.1021/es9000328

Zhou, X., Memon, A. G., Sun, W., Fang, F., & Guo, J. (2020). Fluorescent probe for Ag+ detection using SYBR GREEN I and CC mismatch. *Biosensors*, *11*(1), 6. https://doi.org/10.3390/bios11010006